Copyright Warning & Restrictions

The copyright law of the United States (Title 17, United States Code) governs the making of photocopies or other reproductions of copyrighted material.

Under certain conditions specified in the law, libraries and archives are authorized to furnish a photocopy or other reproduction. One of these specified conditions is that the photocopy or reproduction is not to be "used for any purpose other than private study, scholarship, or research." If a, user makes a request for, or later uses, a photocopy or reproduction for purposes in excess of "fair use" that user may be liable for copyright infringement,

This institution reserves the right to refuse to accept a copying order if, in its judgment, fulfillment of the order would involve violation of copyright law.

Please Note: The author retains the copyright while the New Jersey Institute of Technology reserves the right to distribute this thesis or dissertation

Printing note: If you do not wish to print this page, then select "Pages from: first page # to: last page #" on the print dialog screen

ABSTRACT

MULTICODES FOR IMPROVED RANGE RESOLUTION IN RADAR

by
Rhiya Vitto

Third generation (3G) wireless systems are required to support a variety of communication services like voice, image, motion picture transmission, etc, each of which requires different transmission rates. Multi-code modulation has been introduced therefore as a means of supporting multi-rate services and operating in multi-cell environments [8, 9, 10]. This multi-rate multi-function capability may be used in Radar related applications, too. For example, a single transmitted waveform consisting of two orthogonal codes can be used to simultaneously track a target and obtain high range resolution. Tracking requires low bandwidth and high resolution needs a high bandwidth signal. Orthogonal codes like Walsh codes can be used to provide multiple rates if the codes are chosen from the same matrix, because certain Walsh codes of the same length have very different bandwidths. Therefore, as an extension to its use in communication, multi-codes can be used to enable multi-function operations in a Radar system.

The first criterion for choosing a Radar waveform, whether single or multi-code, is its resolving capability in range and Doppler. A measure of range resolution or sensitivity to delay commonly used in Radar literature is the Peak to Sidelobe Level Ratio (PSLR) of the code's autocorrelation function. The multi-codes proposed in this work are found to have better (lower) PSLRs than existing radar codes when the number of simultaneously transmitted codes is large. In the special case of using an entire set of orthogonal codes of any length, the resulting multi-code consists of just a single pulse of

thickness equal to the chip width of the code used. This pulse will have a 'perfect' autocorrelation function with only a single peak at the main lobe and zero sidelobes. This gives the ideal PSLR for radar purposes.

An important aspect of using multi-codes in Radar is the need for multiple transmitters to avoid the high peak factor that would result if only a single antenna is used. This requires the Radar system to have multiple transmitters as in phased array radar. The best example is a multi-function digital array radar that transmits a unique orthogonal code from each of its antenna elements as described by Rabideau and Parker in [13]. The system described in this publication makes use of the array mode of operation of the Radar to transmit orthogonal codes from each antenna element which are then phased and combined at the receiver. The phase (or angle) of the signal at each receive antenna element can be used to better resolve targets that are spatially separated.

This thesis introduces the concept of multicodes in Radar. Further, the advantages of using multiple coded waveforms over the known Radar polyphase codes are demonstrated by simulations.

MULTICODES FOR IMPROVED RANGE RESOLUTION IN RADAR

by
Rhiya Vitto

A Thesis
Submitted to the Faculty of
New Jersey Institute of Technology
in Partial Fulfillment of the Requirements for the Degree of
Master of Science in Electrical Engineering

Department of Electrical and Computer Engineering

August 2005

APPROVAL PAGE

MULTICODES FOR IMPROVED RANGE RESOLUTION IN RADAR

Rhiya Vitto

Dr. Alexander M. Haimovich, Thesis Advisor — Date
Professor of Electrical and Computer Engineering, NJIT

Dr. Ali N. Akansu, Committee Member — Date
Professor of Electrical and Computer Engineering, NJIT

Dr. Roy R. You, Committee Member — Date
Assistant Professor of Electrical and Computer Engineering, NJIT

BIOGRAPHICAL SKETCH

Author: Rhiya Vitto

Degree: Master of Science

Date: August 2005

Undergraduate and Graduate Education:

- Master of Science in Electrical Engineering,
  New Jersey Institute of Technology, Newark, NJ, 2005

- Bachelor of Engineering in Electronics and Communication Engineering,
  University of Madras, Madras, India, 2003

Major: Electrical Engineering

To My Dear Little Sister

ACKNOWLEDGEMENT

I would like to express my deepest gratitude to Dr. Alexander M. Haimovich, who as my research advisor provided invaluable insight into the basic concepts involved in my work and for his constant guidance, support, encouragement and reassurance.

I thank Dr. Ali Akansu and Dr. Roy You for their active participation in my thesis evaluation committee.

I am greatly indebted to Mr. Nikolaus Lehmann for his immense help in debugging a part of the code, clearing up many doubts and for helping me understand some important concepts during the course of this research.

Finally, I wish to give special thanks to Mrs. Marlene Toeroek for all her help during the period of time I worked at the CCSPR.

TABLE OF CONTENTS

TABLE OF CONTENTS
(Continued)

TABLE OF CONTENTS
(Continued)

Chapter **Page**

LIST OF FIGURES

LIST OF FIGURES
(Continued)

CHAPTER 1

INTRODUCTION

In this chapter, a brief introduction to Radar systems and the classifications of Radar is given. The two types of Radar systems that may be used to transmit multicodes – the phased array radar and MIMO radar, are also discussed. The matched filter receiver, which is an important part of a Radar, and its similarity to a correlation receiver, is also explained in brief.

1.1 Basic Radar Operations

RADAR is an abbreviation for Radio Detection And Ranging. Radar was first developed as a device to detect a target and measure its range. RADAR systems perform two basic operations: (1) detecting the target and (2) extracting information like position, velocity, shape, etc from the received waveform. The problem of detection depends mostly on the received signal's energy compared to the noise level and less on the waveform itself. The type of waveform used determines the accuracy, resolution and ambiguity associated with obtaining the target's range and radial velocity [2].

The range is associated with the delay of the received signal and the radial velocity with its Doppler shift. The range of the target is determined by measuring the time taken for the Radar signal to travel to the target and back. The velocity of the target is measured using the relative shift in carrier frequency of the reflected wave, termed as the Doppler effect. This can be used to distinguish moving targets from stationary ones

or to distinguish more than one moving targets. The Doppler can also be used to distinguish a target from its surrounding clutter.

1.2 Classifications of Radar

Radars are classified based on different criteria. They can be ground-based, airborne, space borne, or ship based radar systems. Based on the functionality they can be classified as weather, acquisition and search, tracking, track-while-scan, fire control, early warning, over the horizon, terrain following and terrain avoidance Radars. Radars can also be classified based on specific radar characteristics like frequency band, antenna type, waveforms utilized, etc [16].

The necessity for obtaining information about many targets at a flexible, rapid data rate and the need to shift the scanning beam rapidly from one position in space to another using beamforming techniques [1], led to the development of phased array radars. Later, more recently, this has been extended to MIMO Radar. Other forms of antenna systems include multiple-input-single-output (MISO) and single-input-multiple-output (SIMO) radars [17]. Phased array radars can be considered to be a type of MIMO Radar, but even though both use multiple transmit and/or receive antennas, there are fundamental differences in their antenna systems and in their functionalities that are explained in the following sections.

1.3 Phased Array Radar

A phased array resembles a directive antenna that consists of many radiating antenna elements. Each element generates a radiation pattern whose shape and direction is determined by the relative phases and amplitudes of the currents at the individual elements. Beam steering is the process of rapidly steering the beam of an array antenna in space by properly varying the phase of the signals applied to each element. In an electronically scanning array, the phase shift between the elements is controlled by electronic devices. This was a major improvement over the mechanical phase shifters because of the lack of mechanical elements in the system, the ability to use advanced signal processing techniques to improve performance, etc.

In phased array radars, the antenna elements are closely spaced so that the transmitted waveform illuminates only one aspect of the target. In other words, each of the transmit beams from the radiating antennas sees the same aspect of the target and hence the waveforms at each receive antenna have the same gain. This is the basis for the transmission of multicodes in this thesis because at the receiver, the individual codes in the received waveform are not exposed to different Radar Cross Sections (RCS) of the target. The multicodes considered here are assumed to be transmitted from a phased array radar where each code sees the same aspect of the target and so has the same gain at the receiver. Section 3.2.3 talks about a phased array radar system as described by Rabideau et al [13], which is used to obtain the angular resolution of spatially separated targets.

1.4 MIMO Radar

MIMO radar differs from phased array radar mainly in that the transmit and receive antenna elements are spaced far apart when compared to phased arrays, where they are closely spaced. Each of the radiating elements views a different uncorrelated aspect of the target [18]. Phased arrays use beamforming to cohere a beam towards a direction in space and obtain a coherent processing gain. These systems are prone to target fading. MIMO Radar exploits the target angular spread and realizes a spatial diversity gain to overcome target fading and improve detection performance [17]. Since each antenna element sees a different aspect of the target, the received waveforms at each receive antenna undergo different gains.

1.5 Matched Filter Receiver

The matched filter has a frequency response function that maximizes the output peak signal to noise ratio. This is the criterion used for the design of most radar receivers. The frequency response of a linear time-invariant filter that maximizes the output peak signal to noise power for a fixed input signal to noise ratio is given by:

$$H(f) = S^*(f)\exp(-j2\pi f t_1) \tag{1.1}$$

where

$$S(f) = \int_{-\infty}^{\infty} s(t)\exp(-j2\pi ft)dt = \text{ spectrum of the input signal}$$

$S^*(f) =$ complex conjugate of $S(f)$

t_1 = fixed value of time at which signal is observed to be maximum

The matched filter can also be specified by its impulse response, which is the inverse Fourier transform of its frequency response:

$$h(t) = \int_{-\infty}^{\infty} H(f)\exp(j2\pi ft)df \tag{1.2}$$

From (1.1) and (1.2) it can be seen that,

$$h(t) = \int_{-\infty}^{\infty} S^*(f)\exp\left[-j2\pi f\left(t_1 - t\right)\right]df \tag{1.3}$$

Since $S^*(f) = S(-f)$,

$$h(t) = \int_{-\infty}^{\infty} S(f)\exp\left[j2\pi f\left(t_1 - t\right)\right]df = s(t_1 - t) \tag{1.4}$$

This means that the impulse response of a matched filter is equal to the shifted version of the input signal $s(t)$. The output of the matched filter $y(t)$ with impulse response $h(t)$ when the input is $r(t) = s(t) + noise$, is given by:

$$y(t) = \int_{-\infty}^{\infty} r(t-\lambda)h(\lambda)d\lambda \tag{1.5}$$

For the matched filter, $h(\lambda) = s(t_1 - \lambda)$. So (1.5) becomes:

$$y(t) = \int_{-\infty}^{\infty} r(t-\lambda)s(t_1-\lambda)d\lambda$$

$$= \int_{-\infty}^{\infty} r(\lambda)s(\lambda-(t_1-t))d\lambda$$

$$= R(t-t_1) \tag{1.6}$$

where $R(t) = \int_{-\infty}^{\infty} y(\lambda)s(\lambda-t)d\lambda$ is the cross-correlation of two signals $y(\lambda)$ and $s(\lambda)$ each of finite duration.

Thus from (1.6), it is obvious that the matched filter output is equal to the cross-correlation of the input signal and a delayed version of the transmitted signal. Hence the matched filter is equivalent to a cross-correlation receiver mathematically and the choice of which to use for a particular radar application depends on which one is more practical to implement [1].

CHAPTER 2

RADAR WAVEFORM ANALYSIS

In this chapter, the principles involved in designing and choosing waveform for Radar purposes are explained. The tools used to analyze these waveforms in order to obtain target information are also discussed. Finally, this chapter introduces the metrics of measure used to evaluate the system performance, given a particular Radar waveform.

2.1 Pulse Compression

Pulse compression allows Radar to use a long pulse of smaller amplitude to achieve large radiated energy and to simultaneously obtain the range resolution of a short pulse [1]. This is done by frequency or phase modulation to widen the signal bandwidth. Pulse compression achieves most of the benefits of a short pulse while maintaining the practical constraints of the peak power limitation. The two most common forms of pulse compression, linear frequency modulation and phase coding, are described in the following sub-sections.

2.1.1 Frequency Coding

The transmitted waveform is usually a rectangular pulse of constant amplitude whose frequency increases linearly over the duration of the pulse. At the receiver, the frequency modulated signal is passed through a pulse compression filter designed so that the velocity of propagation through the filter is proportional to frequency. The pulse

compression filter speeds up the higher frequencies at the trailing edge of the pulse relative to the lower frequencies at the leading edge. This is equivalent to compressing the pulse to a width 1/B where B is the bandwidth of the pulse. This is linear frequency modulation and the pulse is a Linear Frequency Modulated (LFM) pulse.

2.1.2 Phase Coding

Phase coding is a form of pulse compression of waveforms where a pulse of duration T is divided into M chips of equal duration $t_b = T/M$ and each chip is assigned a different phase value [2]. The main lobe of the output of the matched filter will have a width $2t_b$ and amplitude M times greater than the original pulse. The pulse compression ratio is $M = T/t_b = BT$ where $B = 1/t_b$ is the bandwidth of the pulse. The phase values may be binary (0 or π) as in Barker codes or poly-phased as in Frank, P4, Zadoff-Chu codes, etc. The choice of the phase codes is determined by their performance for particular Radar applications.

2.2 Radar Waveform Analysis

This section discusses the tools used to analyze the performance of Radar waveforms and measure their sensitivity to delay and Doppler. Waveform analysis is necessary for Radar engineers to choose the best waveform for a particular Radar application and this can be done by comparing the performance of various codes in terms of their sensitivity to delay (for range resolution) and Doppler (for velocity resolution) using the tools described in this section.

2.2.1 Ambiguity Function

In RADAR, targets need to be resolved in both range and velocity simultaneously. The ambiguity or uncertainty in resolving one or more targets is a function of both the time delay τ and Doppler frequency shift ν of the target. The ambiguity function is a measure of the uncertainty with which the received waveform can distinguish simultaneously the range and velocity of a target. It is defined as the envelope of the output of the matched filter receiver when the input is a Doppler shifted and delayed version of the original signal, to which the filter is matched [3]. There is quite a bit of inconsistency in the Radar literature on the exact definition of the ambiguity function. It is represented according to [7] as:

$$\left|X(\tau,\nu)\right|^2 = \left|\int_{-\infty}^{\infty} u(t)u*(t+\tau)\exp(2\pi j\nu t)\,dt\right|^2 \tag{2.1}$$

where $u(t)$ is the complex envelope of the signal.

The τ and ν are the difference in range and velocity of any two targets to be resolved separately, and not the actual range and velocity [5]. This argument relates to the problem where a strongly reflecting target may "mask" a second weak target present in the same range cell. If only a single target is to be resolved, τ and ν can be taken to be the difference in range and velocity of that target with respect to a target at the reference position ($\tau = 0$, $\nu=0$).

2.2.2 Interpreting the Ambiguity Diagram

The ideal ambiguity diagram is a single spike of infinitesimal thickness at the origin and zero everywhere else. This implies that the velocity and range of the target can be

determined simultaneously with the highest accuracy and any two targets can be resolved no matter how close they are in range and velocity. However, the Radar waveform would need to have unlimited maximal power. In reality, any signal will have a certain finite maximal power and so the spike in its ambiguity diagram will have a certain thickness enclosing a volume proportional to the energy of the signal. The thickness of this main lobe at the origin is a measure of close target resolvability in delay and Doppler. The size of the surrounding sidelobes or peaks is a measure of the amount of self-clutter and how much a smaller target having a range and velocity close to that of the larger one may be masked [4]. The lower the sidelobes, the lesser the probability that a smaller target in that range will be masked and the higher will be the range resolution of the target in question.

2.3 Performance Measures Used

In this section, the measures used to determine the performance of various codes in terms of their range and Doppler sensitivity are introduced. These measures help Radar engineers to choose the best code according to its range and/or Doppler resolution depending on the application.

2.3.1 3-D Ambiguity Function

The ambiguity function given in (2.1) is a function of two variables, the delay and Doppler. This makes it a 3-dimensional plot when both of these parameters are considered. The 3-dimensional ambiguity diagram of a particular waveform is used to

measure the ambiguity in resolution that the waveform provides when reflected by a target at both zero and non-zero velocities. As an example, the ambiguity plot of a length-16 P4 code is shown in Figure 2.1 below:

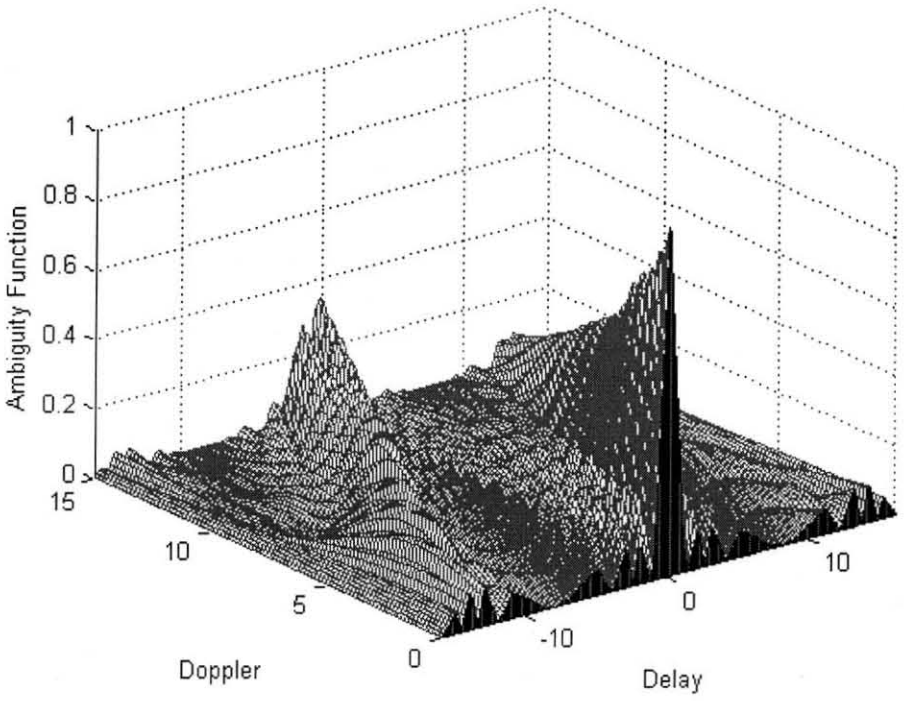

Figure 2.1 Ambiguity plot of a length-16 P4 code.

2.3.2 2-D Ambiguity Function

In some cases, to reduce the complexity of the analysis or if the target under consideration is stationary, the Doppler associated with the ambiguity function of the target is assumed to be zero. Therefore, from (2.1), the zero-Doppler cut of the ambiguity function is given by:

$$\left|X(\tau,0)\right| = \left|\int_{-\infty}^{\infty} u(t)u*(t+\tau)\,dt\right| = \left|R(\tau)\right| \tag{2.2}$$

The ambiguity is now a 2-dimensional plot of the autocorrelation function of the received waveform. It is also the response of the matched filter receiver to a signal arriving with a zero Doppler shift with respect to a reference time. The cut along the delay axis for any other value of Doppler is the response of the matched filter to a signal with the corresponding Doppler shift. For a waveform to have good zero Doppler response, its autocorrelation function must have low sidelobes at non-zero delay values. As an example, the zero-Doppler cut of the ambiguity function of the length-16 P4 code in Figure 2.1 is shown in Figure 2.2.

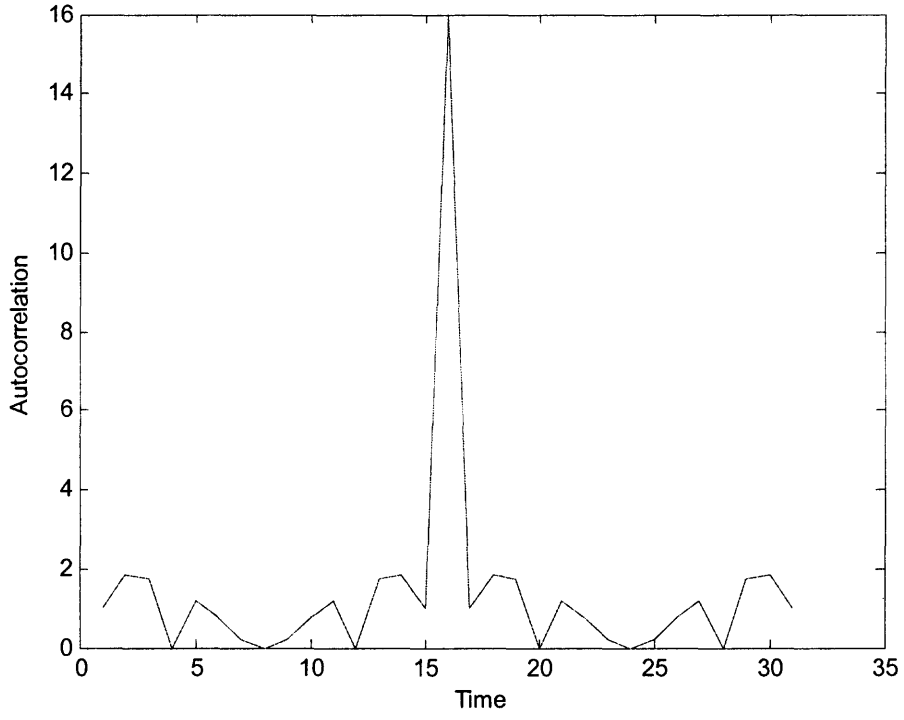

Figure 2.2 Autocorrelation of a length-16 P4 code.

2.3.3 Peak to Sidelobe Level Ratio

RADAR waveforms need to have a narrow main lobe and low sidelobes at both zero and off-zero Doppler. The analysis of the ambiguity function of a waveform is complicated and hence most literature uses only the zero-Doppler response or autocorrelation of the code to describe the sensitivity and resolution capability of a waveform in range. This is measured by the Peak to Sidelobe Level Ratio (PSLR) defined as:

$$\text{PSLR} = \frac{\text{Peak Sidelobe Power}}{\text{Mainlobe Power}} \tag{2.3}$$

The PSLR is the ratio of the power/energy in the highest sidelobe to the power/energy in the main lobe. It follows that for the best ambiguity function, the PSLR of the code used should be as low as possible. Therefore, the code should have low autocorrelation sidelobes.

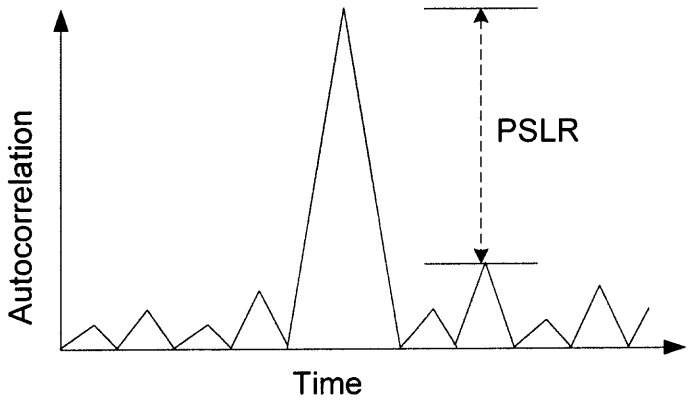

Figure. 2.3 Peak to Sidelobe Level Ratio of the autocorrelation of a code.

CHAPTER 3

MULTICODE MODULATION

This chapter introduces the concept of multicodes. Further, a typical multicode transmission model used in communications is presented. The motivation for the use of multicodes in radar and their advantages are explained, along with a description of the proposed multicode transmission scheme.

3.1 Multicodes in Communication

The demand for multi-user communications systems that can support various communications services like voice, image and motion picture transmission has led to the development of multi-rate systems. 3G wireless systems are required to support multi-rate services like voice, video, data, etc simultaneously. The use of multiple coded waveforms was initially proposed as a means of providing multi-rate services to the evolving second and third generation wireless systems [8]. In multi-code modulation, the high rate data to be transmitted is serial to parallel converted into low rate steams [9, 10].

3.1.1 Multicode Transmission Scheme

In a multicode scheme, additional parallel codes are allocated as the data rate increases. A simplified multicode transmission model is shown in Figure 3.1. The high bit rate data stream is split into N parallel channels, each with data rate R_b. On reception, the data is parallel to serial converted to give the original high rate data stream. Each stream is

encoded by a different orthogonal code and the superposition of all streams is transmitted on a single carrier. The orthogonality can be maintained as the signals propagate over the same path (same delay). However, this hold only for flat fading channels.

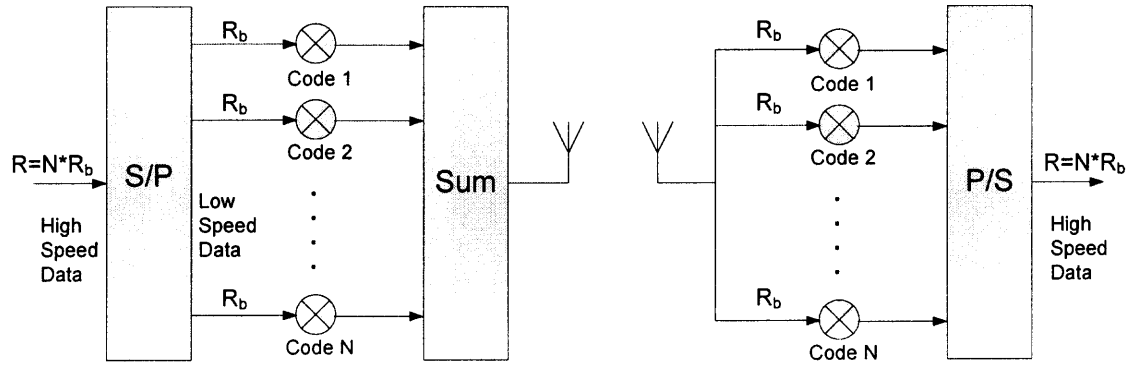

Figure 3.1 Multicode Transmission Scheme

3.1.2 Orthogonal Variable Spreading Factor Codes

In a synchronous CDMA system, the timing of all users is aligned. One set of codes that can be used in a synchronous multicode system is the Orthogonal Variable Spreading Factor (OVSF) codes. The variable spreading factor is realized by considering spreading sequences with different lengths. If Q_j is the sequence length, the jth code sequence is given by [14]:

$$c_j = \left(c_j(0), c_j(1), ..., c_j\left(Q_j - 1\right)\right) \qquad j = 1, 2, ...J \tag{3.1}$$

These codes are orthogonal even when the correlation is carried out among codes of different length, provided the correlation is performed on the window corresponding to the largest spreading factor. Hence the family of codes c_j is orthogonal and has multiple spreading factors. The most well-known family of OVSF codes is the Walsh-

Hadamard code family. Figure 3.2 taken from [14] is a representation of the generation of OVSF codes using a tree.

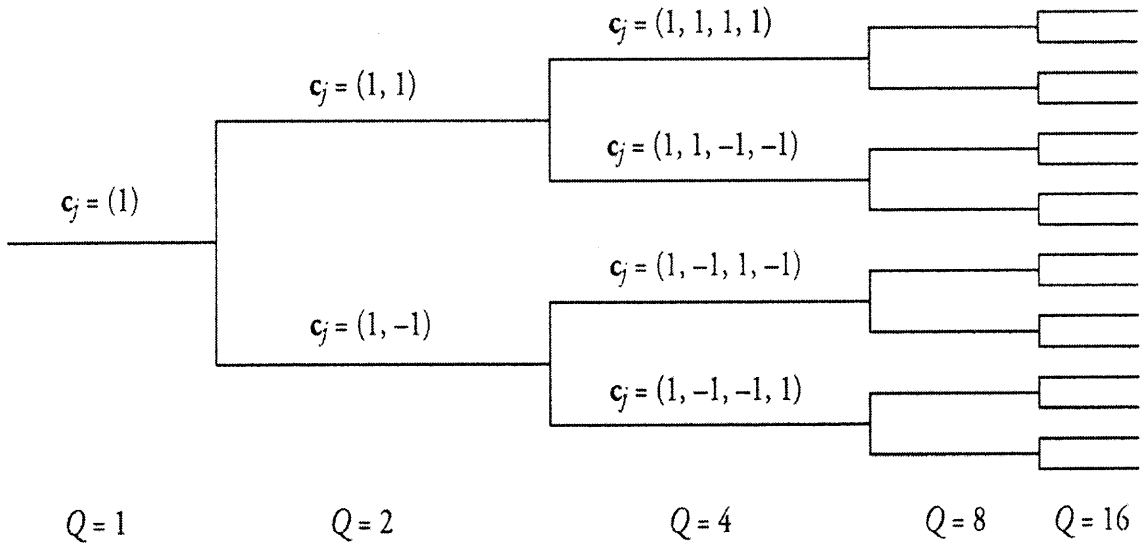

Figure 3.2 Tree for generation of OVSF codes

Each level in the tree defines a spreading factor Q_j. In order to warrant orthogonality, there are certain rules that have been developed for various communication standards which must be followed in the selection of the codes from the tree [19, 20]. Specifically, a particular code can be used if no other code is used in the branches between this code and the root, and if no other code belonging to a branch having the specified code is in use [14]. So, the number of available codes for a multirate transmission depends on the spreading factor and on the number of codes allocated to each spreading factor. Multi-rate OVSF codes provide for multiple functions in a communication system, but over a constant bandwidth because only the code length and hence the data rate is changed, and not the chip duration.

3.2 Motivation for Multicodes in Radar

This section discusses the motivation and potential advantages of using multicodes as Radar waveforms. The main issues that are addressed here are the ability of multiple codes to enable multiple functions by providing for multiple rates and the gain in range resolution obtained by the use of multicodes.

3.2.1 Multifunction Radar

A Radar system differs from a communication system mainly in that there is no 'data' to be modulated in Radar. A Radar waveform is used by itself to provide information about the range and speed of the target. If a single waveform is composed of codes of different bandwidths, each code can be used for a different purpose in a Radar system. For example, precise velocity estimation requires a low bandwidth signal whereas high bandwidth enables precise range estimation of the target. A multicode Radar waveform can have variable bandwidths if the codes used have different pulse-widths. This is similar to communications, except that unlike in communications, there is no 'spreading factor' involved and only the bandwidth of the signal is varied.

The orthogonality of the codes used is a constraint while choosing codes of different bandwidth. For two codes to have different bandwidths and also be orthogonal, they would have to have the same length. This means that the codes chosen must all come from the same matrix of orthogonal codes of the same length. Walsh codes are the only set of codes that can be used to realize this. However, the choice of codes must be made carefully. Consider the Walsh matrix of codes of length 8 given Figure 3.3. The first row that consists of all -1s is a pulse with very small bandwidth, since it is a constant

waveform. The second row in contrast is oscillating and thus, has a much wider bandwidth than the first row. In this manner, carefully chosen codes from the same matrix can provide multiple-bandwidth codes. This would allow for multiple functions to be performed using the same multicode waveform, with each function requiring a signal with a different bandwidth.

$$\begin{bmatrix} -1 & -1 & -1 & -1 & -1 & -1 & -1 & -1 \\ -1 & 1 & -1 & 1 & -1 & 1 & -1 & 1 \\ -1 & -1 & 1 & 1 & -1 & -1 & 1 & 1 \\ -1 & 1 & 1 & -1 & -1 & 1 & 1 & -1 \\ -1 & -1 & -1 & -1 & 1 & 1 & 1 & 1 \\ -1 & 1 & -1 & 1 & 1 & -1 & 1 & -1 \\ -1 & -1 & 1 & 1 & 1 & 1 & -1 & -1 \\ -1 & 1 & 1 & -1 & 1 & -1 & -1 & 1 \end{bmatrix}$$

Figure 3.3 8x8 Matrix of Walsh Codes.

3.2.2 Higher Range Resolution

The first criterion for choosing a Radar waveform, whether single or multi-code, is its resolving capability in range and Doppler. As explained in the previous chapter, the peak to sidelobe level ratio is a measure of a code's range resolution capability. The multicodes proposed in this work are found to have better (lower) PSLRs than existing radar codes when the number of simultaneously transmitted codes is large. In the special case of using an entire set of orthogonal codes of any length, the resulting multi-code has an autocorrelation function that has zero sidelobes as will be explained in Chapter 5.

3.2.3 Angular Resolution of Spatially Separated Targets

A possible implementation of multicodes in Radar systems would be as described in [13], which considers either a phased array radar or a MIMO radar to transmit multiple orthogonal codes from an array of transceivers. In the case of phased arrays, every code sees the same aspect of the target whereas in MIMO radar, they illuminate different aspects of the target because the spatial separation of the transmit antennas is more than in phased arrays. The scheme that is considered in the use of multicodes in this thesis assumes a phased array radar system, because the each of the codes illuminate the same target radar cross section (RCS) and hence have the same gains at the receiver. Thus, multicodes can be used to obtain angular resolution of targets by transmitting the codes from an array of radiating elements as described by Rabideau et al.

3.3 Multicode Radar Transmission

The multicoded waveform is transmitted from a phased array radar system, with each transmit antenna transmitting one, or as many codes as its amplifiers can handle according to their peak power specification. This avoids the high peak power load on the amplifiers that would be present if only a single transmitter is used to transmit many codes. At the receiving end, the receiver correlates on each of the codes. The output of each correlator is the autocorrelation of the corresponding code. Figure 3.4 shows the receiver schematic for a multicode signal formed from four codes as:

$$m(t) = c_1(t) + c_2(t) + c_3(t) + c_4(t)$$

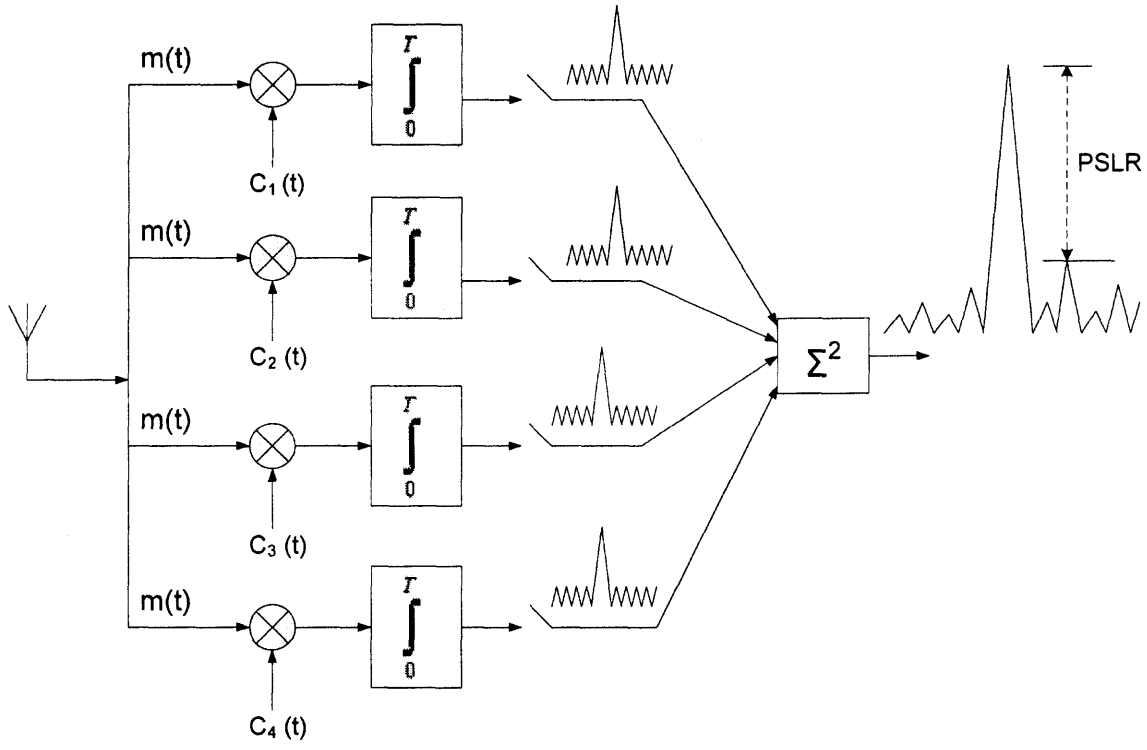

Figure 3.4 Receiver schematic for a 4-code multicode signal m(t)

3.4 Peak Power of Multicodes

The peak to average power ratio (PAPR) or Peak Factor of a signal is defined as:

$$\text{PAPR} = \frac{\text{Peak Power}}{\text{Average power}} = \text{Peak Factor} \tag{3.2}$$

Since multiple codes are used, the peak to average power ratio (PAPR) of the signal comprising the superposition of these codes is proportional to the number of codes used and can be quite high. The PAPR of a signal should be kept as low as possible to avoid exceeding the linearity specifications of the amplifiers in the transmitter. Hence each code is transmitted from a separate antenna, thus avoiding the high peak power that would otherwise be present if just a single transmit antenna is used.

3.5 PSLR Reduction

The statistics of the simulation results show that in some cases, the main lobe of the autocorrelation at the output of the correlation receiver adds up whereas the sidelobes may either add up or cancel out. This leads to a signal that is peakier than each of the original codes. This in turn translates into a lower peak to sidelobe ratio since the main lobe is now much higher than the sidelobes. Simulations have shown that the PSLR of a multiple coded waveform is lower than that of polyphase codes like P4 and Frank if a relatively large number of codes are used.

CHAPTER 4

WAVEFORM SPREADING CODES

The multicodes considered here are based on either Walsh or Orthogonal Gold codes. The performance of these multicodes is compared to that of single code waveforms including polyphase codes P4 and Frank. The P4 and Frank codes are known to have good zero Doppler PSLRs. This chapter first discusses the generation and properties of the known Radar polyphase codes Frank and P4 codes, the need for orthogonality of the multicodes and finally the generation and properties of these multicodes.

4.1 Polyphase Codes

Polyphase codes have lower autocorrelation sidelobes than biphase codes. Some examples of polyphase codes are polyphase Barker, Frank, P1, P2, P3, P4, Zadoff-Chu, Golomb codes, etc. The drawback of polyphase Barker codes is that even though their autocorrelation sidelobes are low, they have high Doppler sidelobes compared to other polyphase codes. So chirp-like polyphase codes like Frank, P4 and the others which have better Doppler properties were developed. In this work, only Frank and P4 codes are used for comparison, because they have very good zero and off-zero Doppler response among all polyphase codes used in Radar. The elements of these polyphase codes are derived from the phase history of a Linear Frequency Modulated (LFM) pulse [2, 3].

4.1.1 Frank Codes

The elements of the Frank code are defined as:

$$s_{(n-1)L+k} = \exp(j\phi_{n,k}) \quad \textbf{for } 1 \le n \le L \textbf{ and } 1 \le k \le L \tag{4.1}$$

where

$$\phi_{n,k} = 2\pi(n-1)(k-1)/L \tag{4.2}$$

for a square length $M = L^2$. The code values can also be expressed as the elements of an LxL discrete Fourier Transform matrix given by:

$$\begin{bmatrix} 0 & 0 & 0 & \cdots & 0 \\ 0 & 1 & 2 & \cdots & L-1 \\ 0 & 2 & 4 & \cdots & 2(L-1) \\ \vdots & \vdots & \vdots & \cdots & \vdots \\ \vdots & \vdots & \vdots & \cdots & \vdots \\ \vdots & \vdots & \vdots & \cdots & \vdots \\ 0 & L-1 & 2(L-1) & \cdots & (L-1)^2 \end{bmatrix}$$

Figure 4.1 Generalized Frank Matrix.

As an example, a 4x4 Frank matrix is shown in Figure 4.2 below:

$$\begin{bmatrix} 0 & 0 & 0 & 0 \\ 0 & 1 & 2 & 3 \\ 0 & 2 & 4 & 6 \\ 0 & 3 & 6 & 9 \end{bmatrix}$$

Figure 4.2 4x4 Frank Matrix.

The 16 element Frank code is obtained by concatenating the rows of this matrix, multiplying by $2\pi / L$ and then taking the phase value modulo 2π :

$$[0 \quad 0 \quad 0 \quad 0 \quad 0 \quad \pi/2 \quad \pi \quad 3\pi/2 \quad 0 \quad \pi \quad 0 \quad \pi \quad 0 \quad 3\pi/2 \quad \pi \quad \pi/2]$$

The autocorrelation function of a length-36 Frank code is shown in Figure 4.3. From the figure, it is seen that the autocorrelation is zero for displacements of multiples of L since the rows of the Frank matrix are orthogonal.

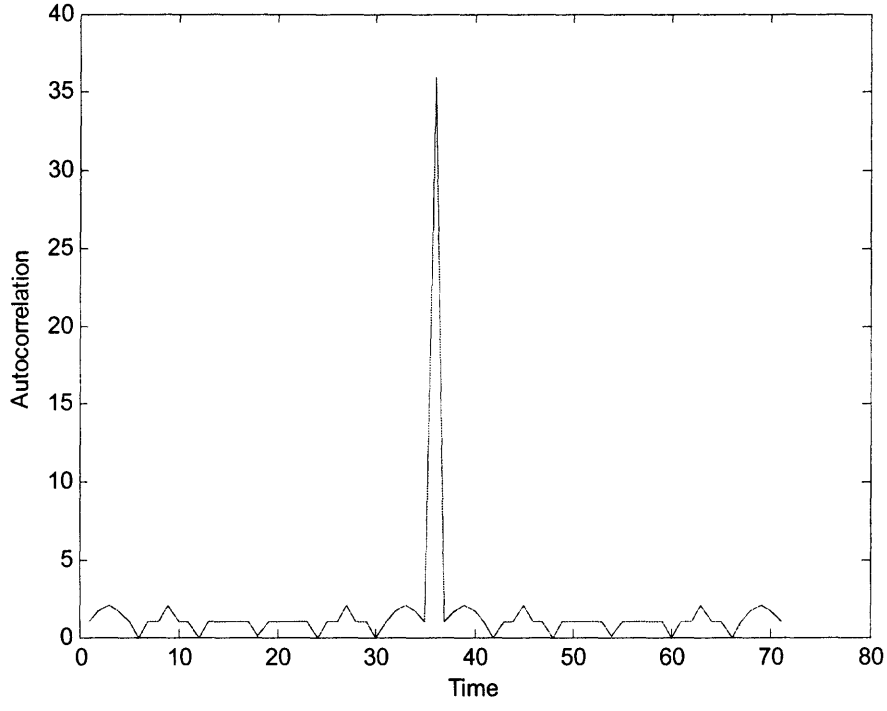

Figure 4.3 Autocorrelation of a length-36 Frank code.

The main drawback of Frank codes is that they exist only for codes of perfect square length $M = L^2$.

4.1.2 P4 Codes

The P4 codes are cyclically shifted and decimated versions of the Zadoff-Chu code whose elements are given by [2]:

$$s_m = \exp(j\phi_m) \tag{4.3}$$

where:

$$\phi_m = \frac{2\pi}{M}(m-1)\left(r\frac{M-1-m}{2} - q\right) \tag{4.4}$$

$1 \le m \le M$, $0 \le q < M$ is any integer and r is any integer relatively prime to M. The phase elements of the P4 code are defined as:

$$\phi_m = \frac{2\pi}{M}(m-1)\left(\frac{m-1-M}{2}\right) \tag{4.5}$$

It can be seen from (4.4) and (4.5) that the P4 code is obtained by setting $r = -1$ and $q = 1$ in the expression for the Zadoff-Chu code. The main advantage of P4 codes is that they exist for any length M unlike Frank codes. But P4 codes have higher Doppler sidelobes than Frank codes.

The autocorrelation function of a length 36 P4 code is shown in Figure 4.4. From Figure 4.3 and Figure 4.4, it can be seen that P4 codes have higher peak sidelobes at zero-Doppler than Frank codes of the same length.

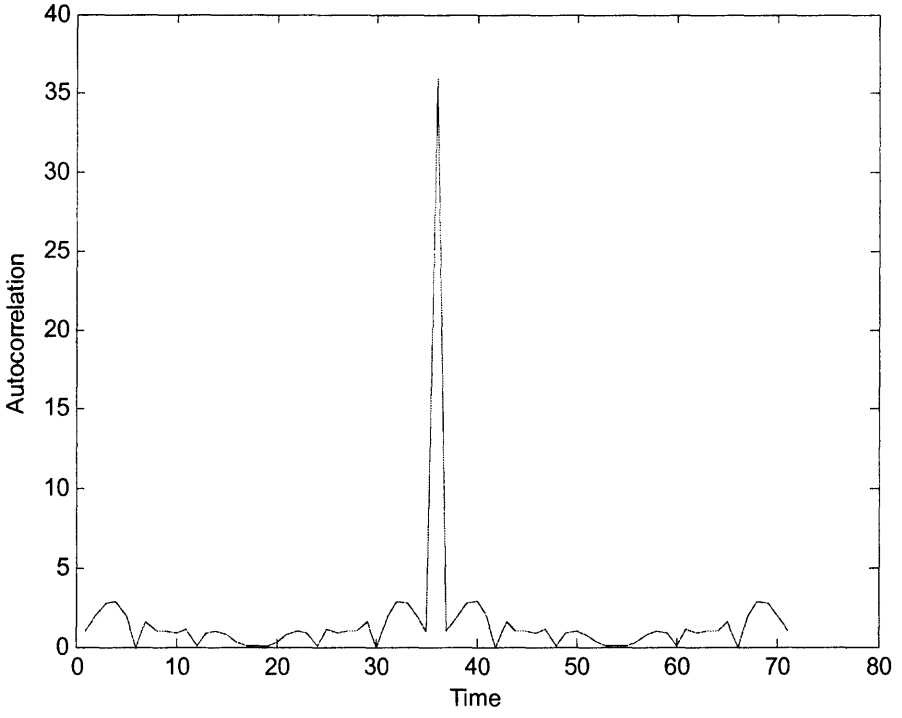

Figure 4.4 Autocorrelation of a length 36 P4 code.

4.2 Orthogonality of Multi-Codes

In mathematics, two vectors are orthogonal if they are perpendicular, i.e., the cosine of the angle between them is zero. Two waveforms are orthogonal if the inner product of the two waveforms taken over a common time period is zero. Thus, two waveforms with complex envelopes $u_m(t)$ and $u_n(t)$ are orthogonal if:

$$\frac{1}{T_b}\int_0^{T_b} u_m(t)u_n^*(t)dt = 0 \tag{4.6}$$

for $m \neq n$ over the interval T_b. The cross-correlation of these two signals is given by:

$$C(\tau) = \frac{1}{T_b} \int_0^{T_b} u_m(t) u_n(t-\tau) dt \qquad (4.7)$$

From (4.6) and (4.7) it follows that two codes are orthogonal if their cross-correlation is null for a zero time shift. Conversely, if two codes are orthogonal they have zero cross-correlation at zero time shift.

The property of zero cross-correlation of certain codes at zero offset is important in multicode communication because it ensures zero interference between each transmitted code. However, the cross-correlation normally does not vanish for non-zero offsets.

4.3 Orthogonal Codes

When transmitting multiple coded waveforms, it is desirable that the codes used are orthogonal to each other to avoid interference among the simultaneously transmitted codes. Therefore Walsh and Orthogonal Gold codes are used as the spreading codes.

Both Walsh and Orthogonal Gold codes have similar cross-correlation functions, but they differ in their autocorrelation functions. Walsh codes have higher autocorrelation sidelobes than Orthogonal Gold codes and hence have a higher PSLR than Orthogonal Gold codes of the same length.

4.3.1 Walsh codes

Walsh codes are generated recursively by applying the Hadamard transform to a one by one dimensional zero matrix repeatedly [11]. The Hadamard transform is given by:

$$H_1 = [0] \tag{4.8}$$

$$H_{2n} = \begin{pmatrix} H_n & H_n \\ H_n & \bar{H}_n \end{pmatrix} \tag{4.9}$$

The Hadamard matrix H_n exists only for $n = 2^i$ where i is an integer. Each column or row is a Walsh code of length n. Every row is orthogonal to all other rows. An example of a length 8 Walsh code is given in Figure 4.5.

$$\begin{bmatrix} 0 & 0 & 0 & 0 & 0 & 0 & 0 & 0 \\ 0 & 1 & 0 & 1 & 0 & 1 & 0 & 1 \\ 0 & 0 & 1 & 1 & 0 & 0 & 1 & 1 \\ 0 & 1 & 1 & 0 & 0 & 1 & 1 & 0 \\ 0 & 0 & 0 & 0 & 1 & 1 & 1 & 1 \\ 0 & 1 & 0 & 1 & 1 & 0 & 1 & 0 \\ 0 & 0 & 1 & 1 & 1 & 1 & 0 & 0 \\ 0 & 1 & 1 & 0 & 1 & 0 & 0 & 1 \end{bmatrix}$$

Figure 4.5 Walsh code matrix of length 8.

During actual transmission of the code, the 0s and 1s are mapped to -1s and 1s. The autocorrelation of a length-16 Walsh code is given in Figure 4.6.

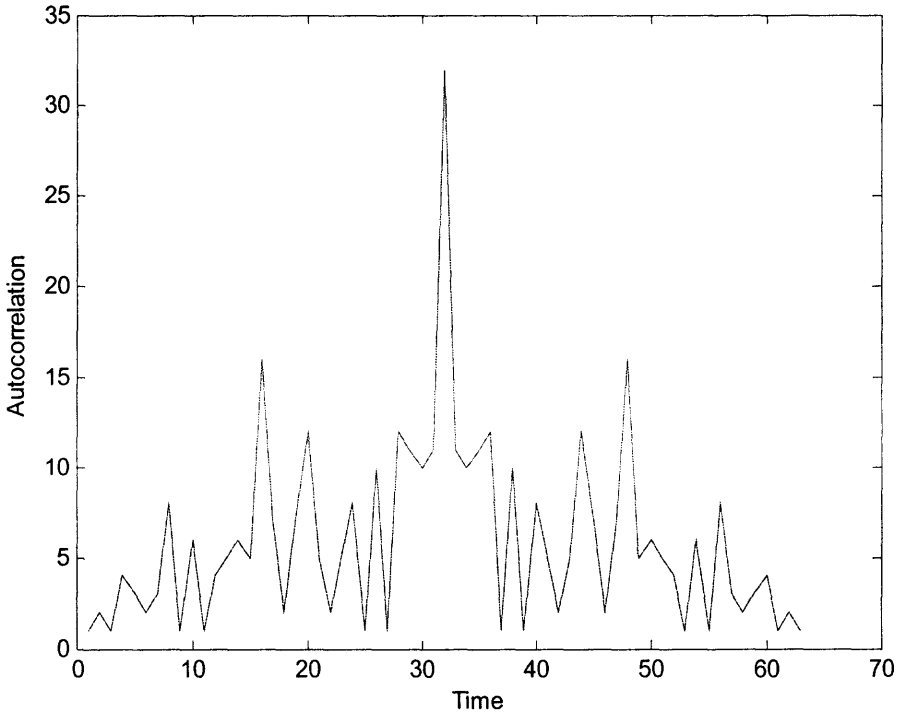

Figure 4.6 Autocorrelation of a length 16 Walsh code.

4.3.2 Orthogonal Gold codes

The cross-correlation values of Gold codes are '-1' for many code offsets. By attaching a '0' to this code, the cross-correlation values associated with these offsets can be made zero [11]. The codes obtained by this zero-padding of Gold codes are called Orthogonal Gold codes.

The Gold code itself is generated from a pair of preferred m-sequences (maximal length sequences) of period $N = 2^n - 1$ where n is the length of the Linear Feedback Shift Register (LFSR). Preferred pairs of polynomials are those that generate a preferred pair of m-sequences that have a three-valued cross-correlation function. The polynomial can be defined as:

$$h(x) = h_0 x^n + h_1 x^{n-1} + ... + h_{n-1} x + h_n \tag{4.10}$$

where $h_i \in (0,1)$ and $h_0 = h_n = 1$. An example polynomial is $x^4 + x + 1$. The coefficients h_i of this polynomial can be represented by binary vectors 10011, or in octal notation as 23. Examples of preferred pairs of polynomials for Gold codes of selected lengths are given in Table 4.1 taken from [15].

Table 4.1 Preferred pair polynomials for Gold codes

Gold Code Length $N = 2^n - 1$	Degree of polynomial n	Preferred Pairs	
		Binary Form	Octal Form
31	5	100101 111101	45 75
63	6	1000011 1100111	103 147
127	7	10001001 10001111	211 217

These polynomials can be generated using shift registers. An explanation of shift registers as given in [12] is provided here. A binary sequence u is generated by $h(x)$, if for all integers j,

$$h_0 u_j \oplus h_1 u_{j-1} \oplus h_2 u_{j-2} \oplus .... \oplus h_n u_{j-n} = 0 \tag{4.11}$$

where $\oplus$ indicates addition modulo 2. If the variables are changed as $j \rightarrow j+n$ and $h_0 = 1$, (4.11) becomes:

$$u_{j+n} = h_n u_j \oplus h_{n-1} u_{j+1} \oplus .... \oplus h_1 u_{j+n-1} \tag{4.12}$$

Here, u_j is the jth bit (called chip) of the sequence u. Equation (4.12) shows that the sequence u can be generated by an n-stage linear feedback shift register which has a feedback tap connected to the ith cell if $h_i = 1, \quad 0 < i \leq n$. As an example, for $n = 5$, (4.12) becomes:

$$u_{j+5} = h_5 u_j \oplus h_4 u_{j+1} \oplus h_3 u_{j+2} \oplus h_2 u_{j+3} \oplus h_1 u_{j+4} \tag{4.13}$$

As an example, the LFSR for polynomial 45 from Table 4.1 is given below:

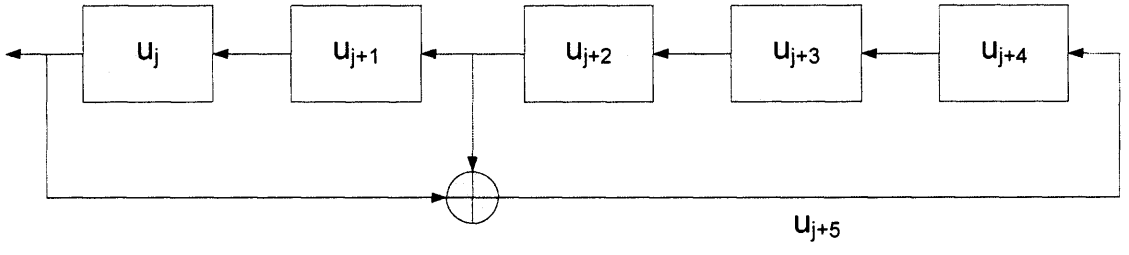

Figure 4.7 Linear Feedback Shift Register for polynomial 45.

$N+1$ or 2^n Gold codes of length $N = 2^n - 1$ are obtained using two LFSRs as shown in Figure 4.8 taken from [11], by changing the value of one of the LFSRs from 0 to $2^n - 1$. An additional Gold sequence is obtained by setting the values of the other LFSR to all zeros. Hence a total of $N+2$ or $2^n + 1$ Gold sequences can be obtained for a code length of N.

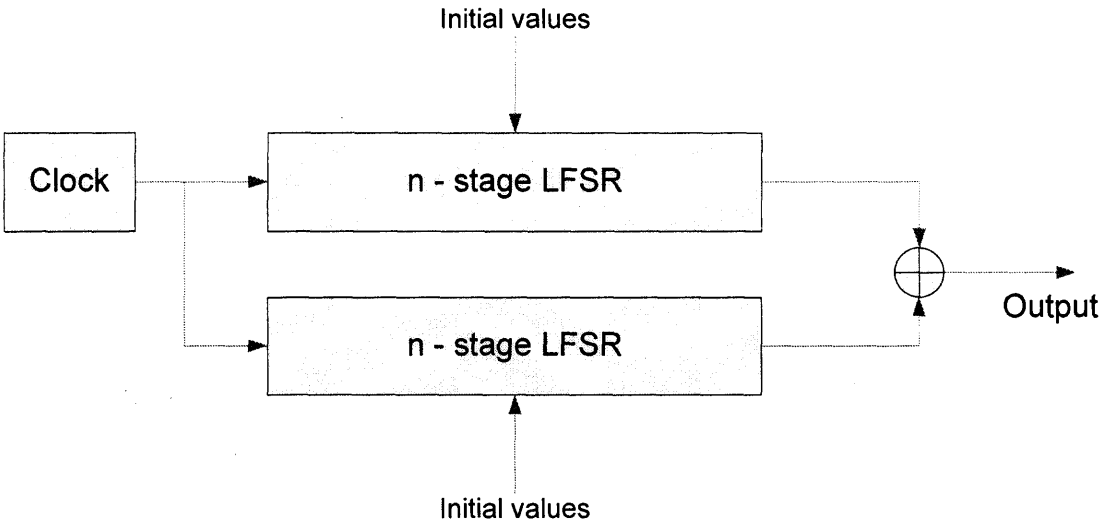

Figure 4.8 Gold code generator.

The Gold codes explained above exist only for $n \neq 0 \bmod 4$. When $n = 0 \bmod 4$, the cross-correlation function is 4-valued [12] and the codes are called Gold-like codes which are not optimal. Hence the Orthogonal Gold codes are constructed only from Gold codes of lengths $N = 2^n - 1$, where n is not a multiple of 4. In other words, Gold codes and hence Orthogonal Gold codes do not exist for lengths 16, 256, etc.

During actual transmission of the code, the 0s and 1s are mapped to 1s and 1s. The autocorrelation of a length-16 Gold code is shown in Figure 4.9.

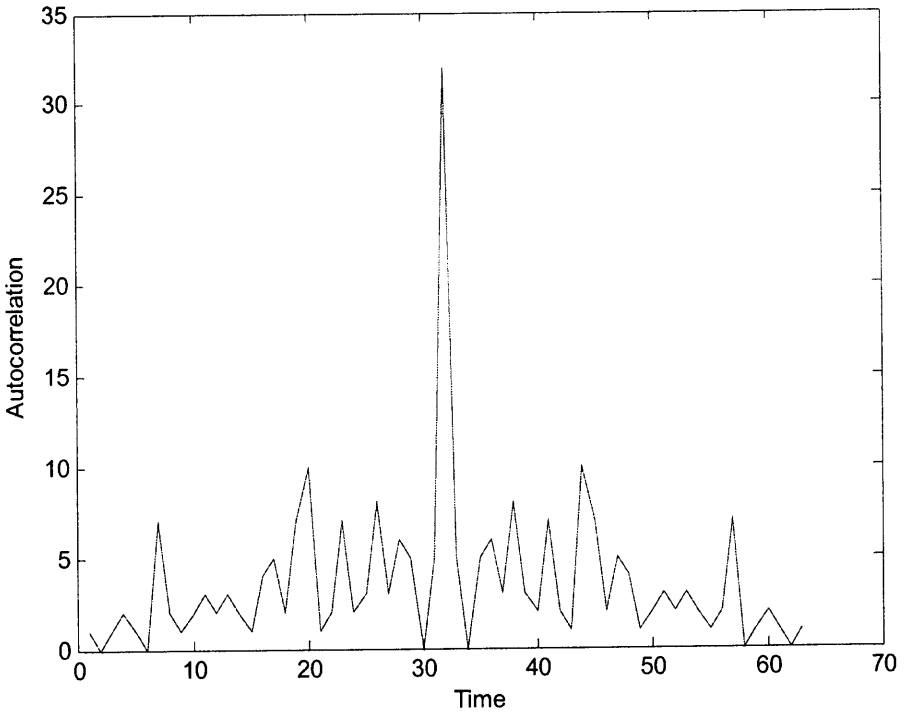

Figure 4.9 Autocorrelation of a length 16 Orthogonal Gold code.

CHAPTER 5

PERFORMANCE OF PROPOSED MULTICODES

In this chapter, the performance of the proposed multicodes in terms of the PSLR is discussed. It is shown that for a relatively large number of codes, the PSLR is lower than that of polyphase codes P4 and Frank. The PSLR is found for both partial and full set multicodes and the inferences from the results are also discussed.

5.1 P4 and Frank Codes

The PSLR values of P4 and Frank codes for the different code lengths considered here are provided in Table 5.2. The properties of the multicodes based on Orthogonal Gold and Walsh codes are explored in this thesis by comparing their PSLRs values to those of P4 and Frank codes.

Table 5.1 Peak Sidelobe Level of P4 and Frank codes

Code Length	**PSL (dB)**	
	P4	**Frank**
16	-18.75	-21.1
32	-21.6	-25.11
64	-24.36	-27.8
128	-27.4	-30.74

5.2 Partial Set Multicodes

The spreading factor of each code (or code length) is N. The number of possible code sets that can be formed using L codes each of length N is given by:

$$ {}_{N}C_{L} = \frac{N!}{L!(N-L)!} \tag{5.1} $$

These values are shown in Table 5.1 for certain values of N and L.

Table 5.2 Number of possible code sets for different values of N and L

N	L	${}_{N}C_{L}$
32	2	496
32	3	4960
32	4	35690
64	2	2016
64	3	41664
64	4	635376
128	2	8128
128	3	341376
128	4	10668000

As can be seen from the table, for combinations of $N > 32$ and $L > 3$ and for combinations of $N > 64$ and $L > 2$ the number of code sets is too large for the program to be computationally efficient. Therefore, in the PSLR plots that follow, the PSLR for higher N and L are the lowest PSLRs obtained through many iterations of a

random selection of codes. The random selection is done such that no code is chosen twice in the same selection. These are not necessarily the least PSLRs that can be obtained for those values of N and L. The cumulative distribution functions (CDFs) of these code selections obtained by the statistics of the search are also plotted here. For smaller values of N and L, the least value of PSLR over all code set combinations can be found.

The multicodes can be formed using either a few of the codes or the entire set of codes for a given length. The former are referred to as partial and the latter as full-set multicodes in the following discussions. The PSLR of Walsh and Orthogonal Gold multicoded waveforms are plotted along with that of P4 and Frank codes of the same length in the following figures:

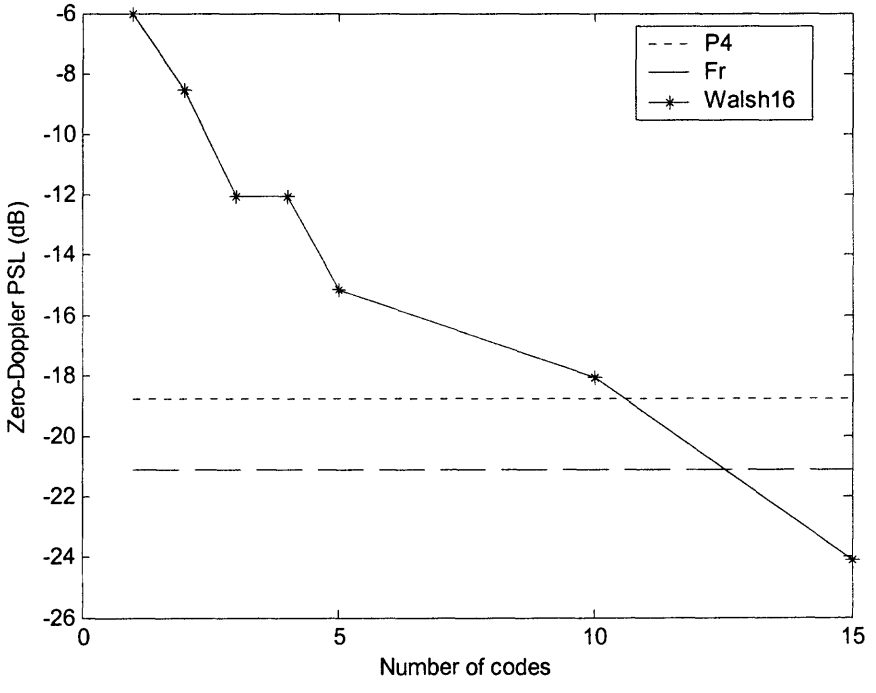

Figure. 5.1 PSLR of length-16 Walsh multicodes.

From Figure 5.1 it can be seen that the PSLR improvement is significant when 15 Walsh codes are transmitted. Since Orthogonal Gold codes do not exist for length 16, only the PSLR of Walsh multicodes are plotted for this length.

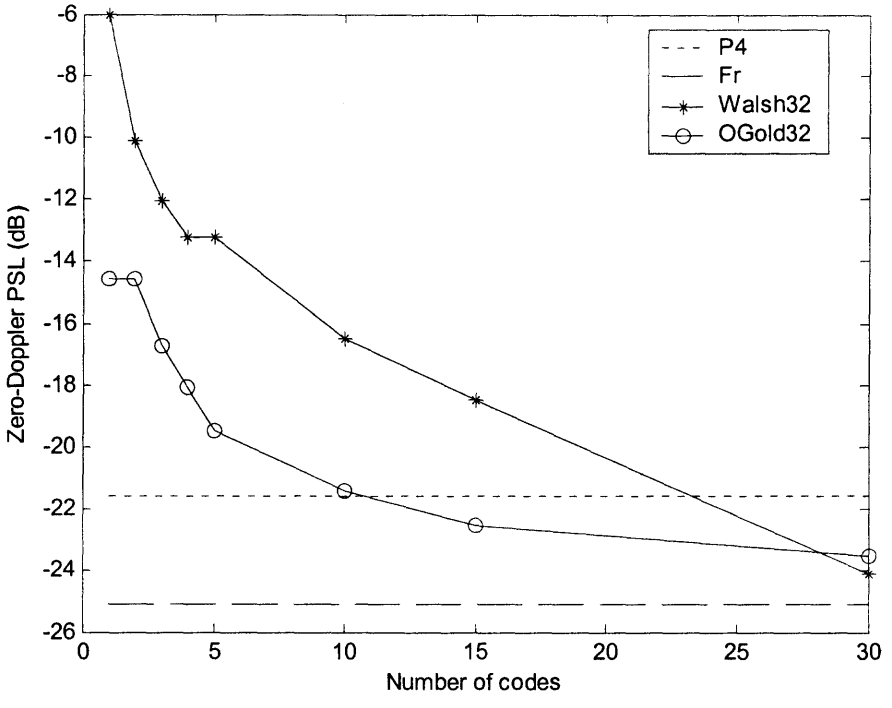

Figure. 5.2 PSLR of length-32 Walsh and O-Gold multicodes.

A point to be noted in Figure 5.2 and the following two figures is that for small number of codes used, Walsh and Orthogonal Gold multicodes have very different PSLRs, with Orthogonal Gold multicodes having the lower values. As the number of codes is increased, this difference is less prominent and both Walsh and Orthogonal Gold multicodes have almost the same values of PSLRs.

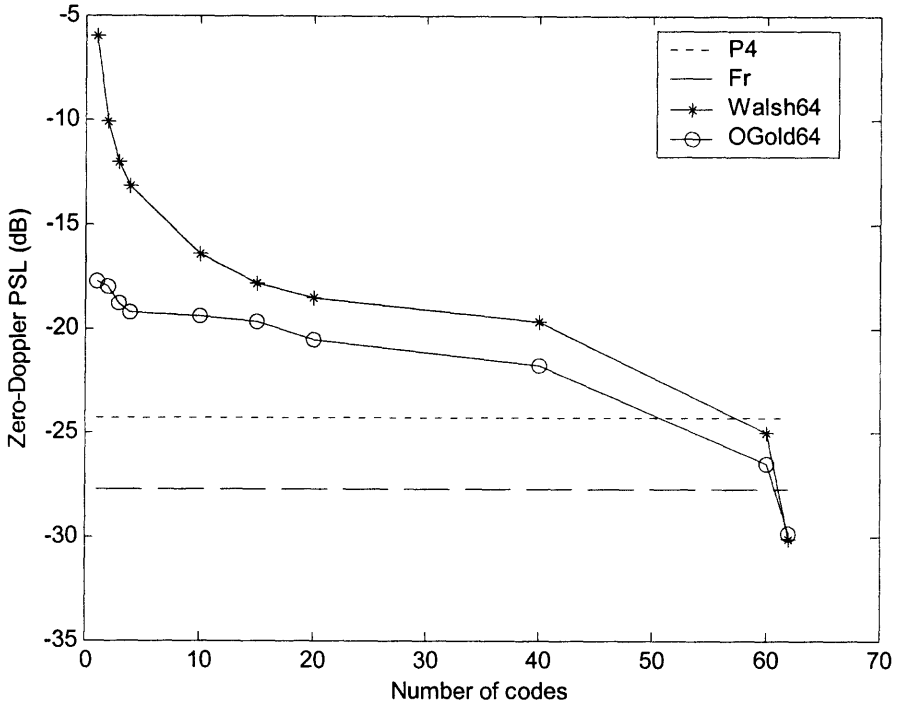

Figure 5.3 PSLR of length-64 Walsh and O-Gold multicodes.

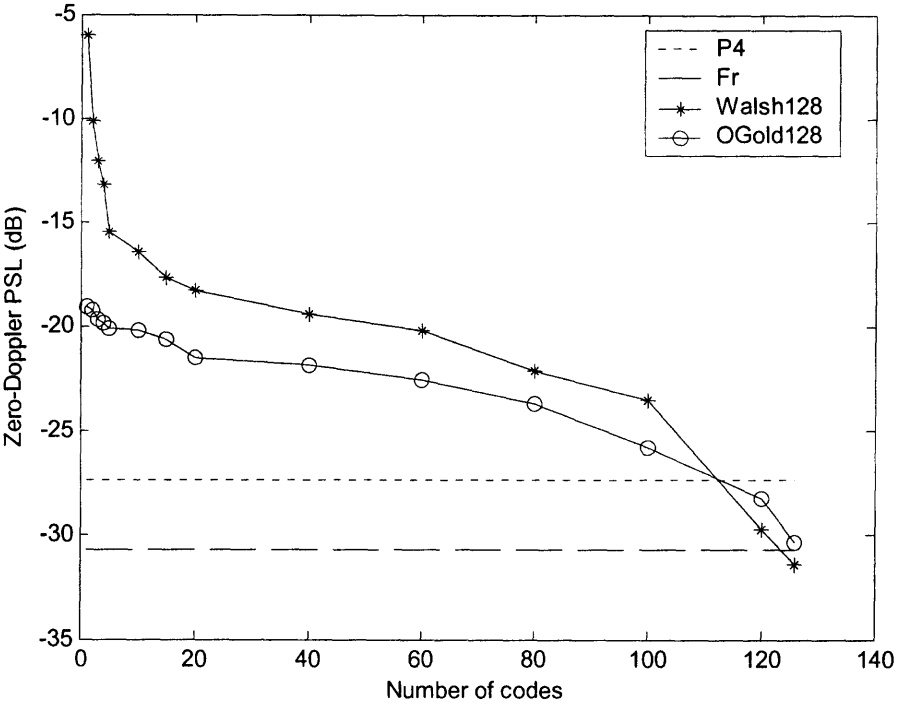

Figure 5.4 PSLR of length-128 Walsh and OGold muticodes.

In the previous plots, only a subset of size L of the total number of codes for a given length N is considered. The first inference that can be made from the simulations is that multicodes perform better than the single codes of Walsh and Orthogonal Gold. From Figure 5.2, Figure 5.3 and Figure 5.4, it can be observed that for any length N, Orthogonal Gold multicodes have lower PSLRs than Walsh multicodes. This difference is because Orthogonal Gold codes have lower autocorrelation sidelobes than Walsh codes. Thus, they have lower PSLRs also.

Also, Figure 5.2 shows that from the results obtained so far for code length 32, Orthogonal Gold multicodes have a lower PSLR than Frank and P4 when the number of codes used is approximately more than 50% of the code length. When the code length is increased, as can be seen from Figure 5.3 and 5.4, the improvement over Frank and P4 codes occurs only when the number of codes used is more than 90% of the code length. It should be noted that these values are only the results of a random choice of codes from the entire set, and the PSLR values can very well be lower if the simulation is performed for all possible code combinations. The CDF plots of the random selections for large number of codes are shown in the following figures.

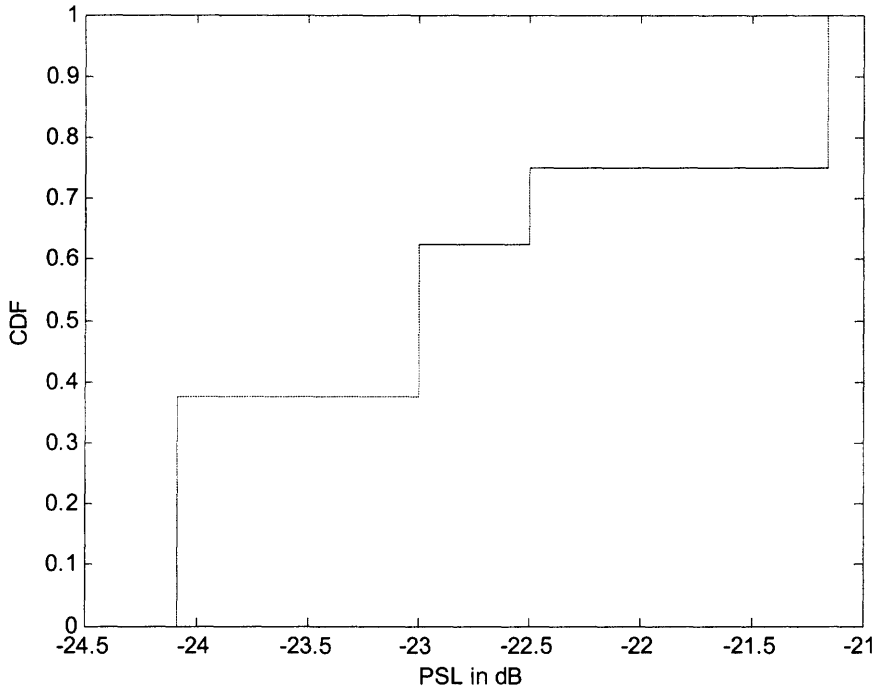

Figure 5.5 CDF plot of PSLR of Walsh multicodes for N=16, L=15.

In Figure 5.5 and the following two figures, the CDF is found for the entire set of codes of that particular length. It can be seen that when the subset of codes transmitted is almost equal to the entire set of codes, the PSLR improvement over Frank and P4 is significant. Also, there exists more than one multicode for the lowest PSLR values found. Specifically, for 15 codes used out of a set of length-16 Walsh codes, almost 40% of the codes have PSLRs much lower than Frank and P4. From Figure 5.6, it can be seen that over 40% of the multicodes have a PSLR much lower than P4 codes.

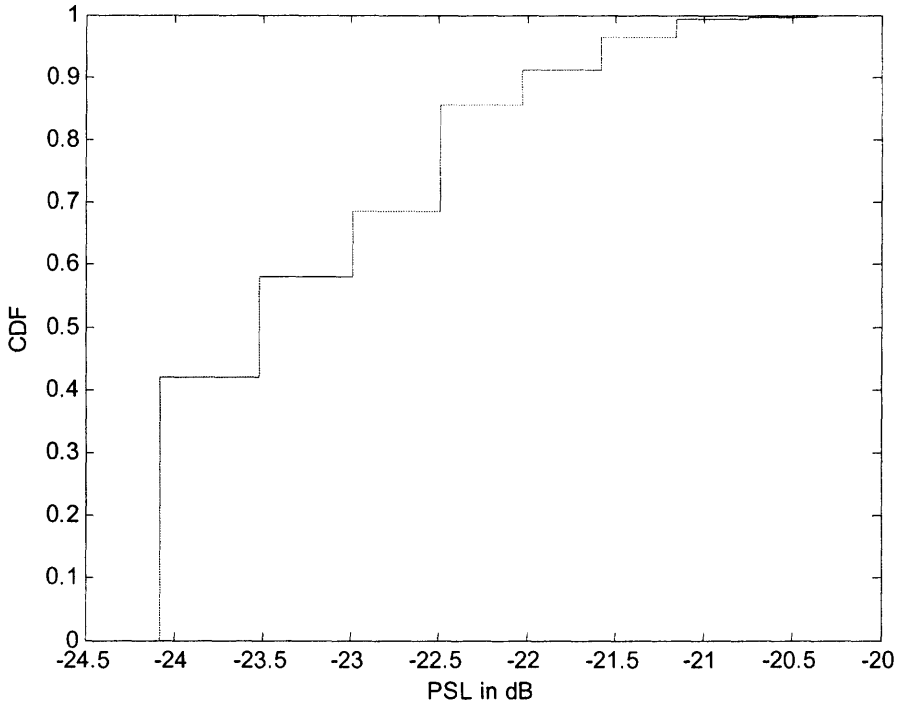

Figure 5.6 CDF plot of PSLR of Walsh multicodes for N=32, L=30.

The percentage of multicodes that have PSLRs lower than Frank codes reduces for larger code lengths as can be seen from Figure 5.7 for a code length of 64 and Figure 5.8 for a code length of 128.

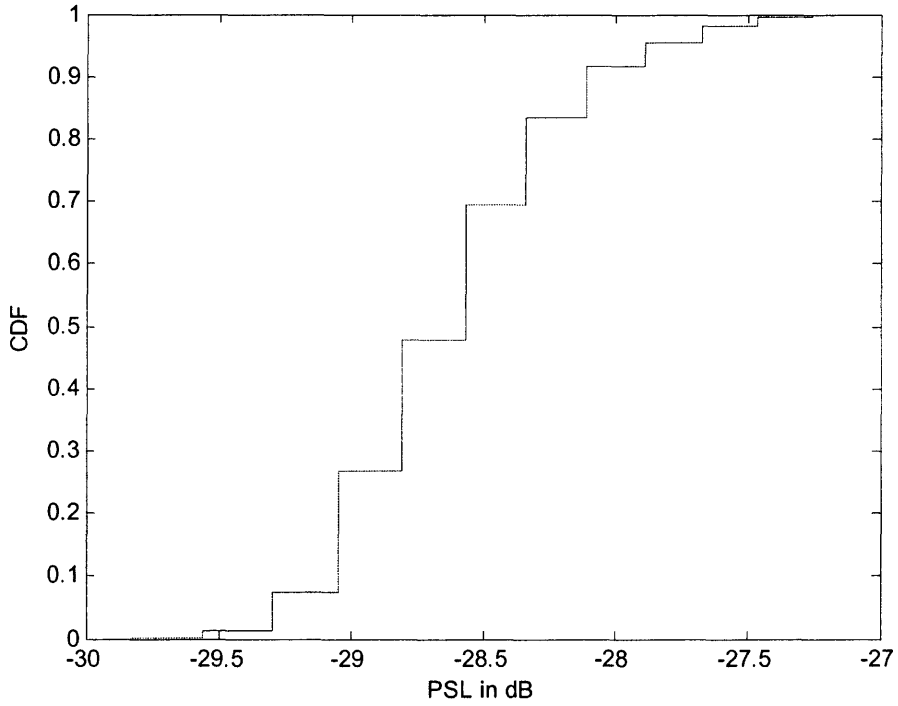

Figure. 5.7 CDF plot of PSLR of Orthogonal Gold multicodes for N=64, L=62.

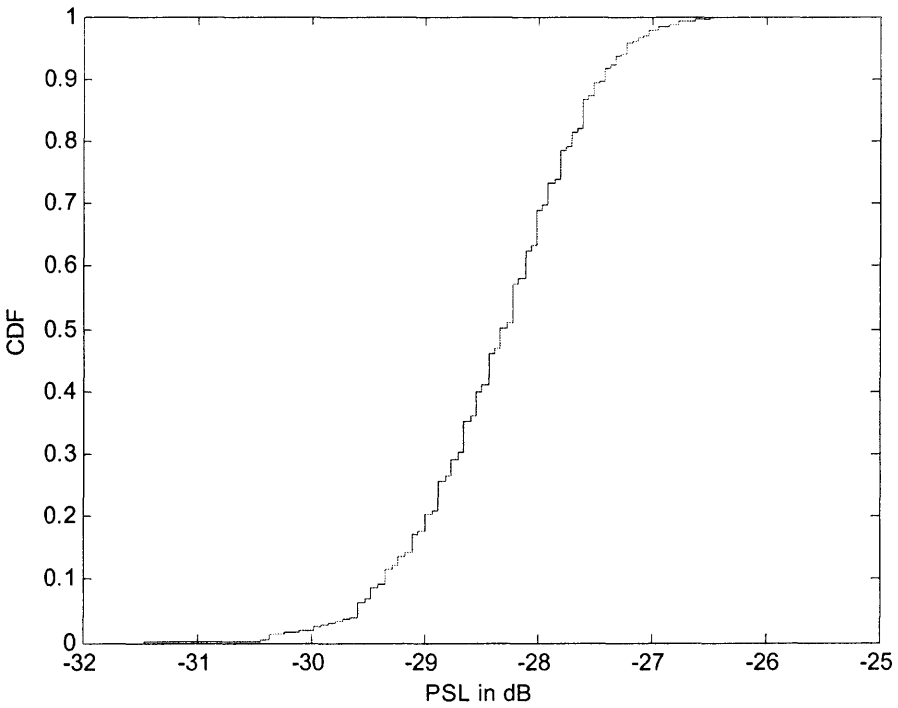

Figure 5.8 CDF plot of PSLR of Walsh multicodes of for N=128, L=126.

The CDF of the random selections of code sets of length 32, 64 and 128 are provided in the following figures. The slope of the CDF plot can be used to estimate the probability of obtaining codes with lower PSLRs than those shown by the CDF plot. This can be observed in Figure 5.9, where the slope is more compared to the CDF plot of Figures 5.10 and 5.11. The probability of finding multicodes with PSLRs lower than the lowest value in the plots is more in Figure 5.9 below, when compared to Figures 5.10 and 5.11.

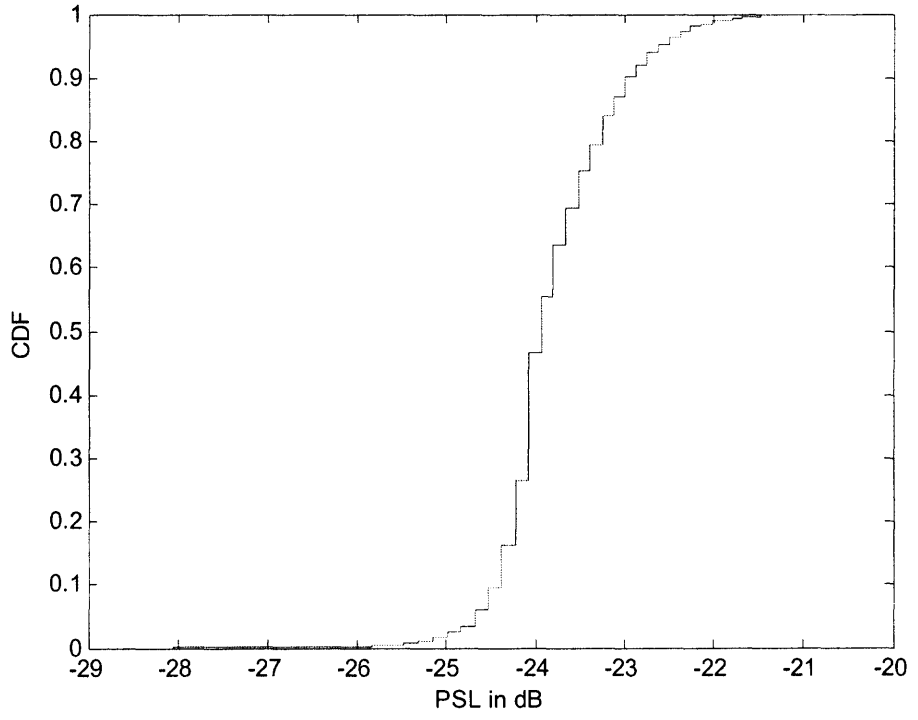

Figure 5.9 CDF plot of PSLR of O-Gold multicodes of for N=64, L=60.

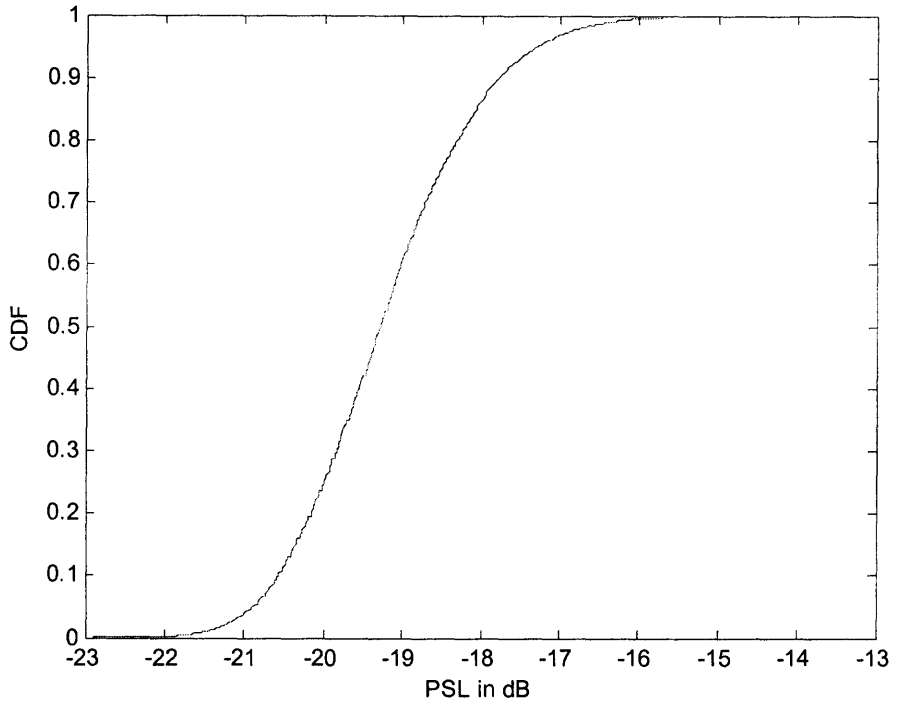

Figure 5.10 CDF plot of PSLR of O-Gold multicodes of for N=128, L=100.

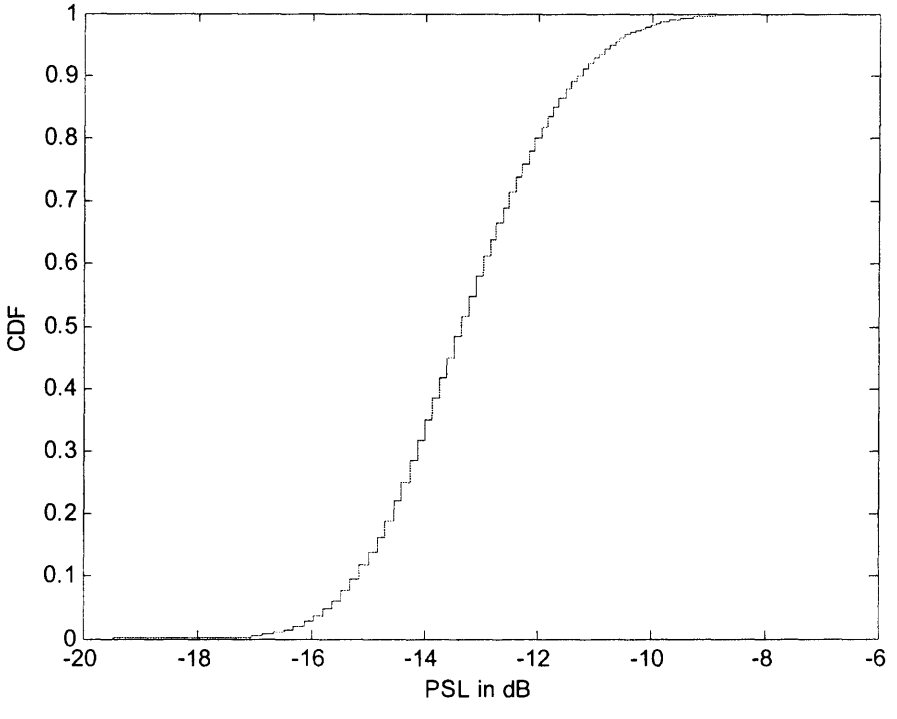

Figure 5.11 CDF plot of PSLR of Walsh multicodes of for N=64, L=20.

5.3 Full Set Multicodes

The superposition of the entire set of orthogonal codes of any length N is equal to a single pulse of amplitude N. Therefore, the autocorrelation or zero-Doppler ambiguity function consists of a single peak of height N^2 at the main lobe with a thickness equal to the pulse width. An example is shown in Figure 5.12 for the full set of a multicode formed from Walsh codes of length 8:

$$
\begin{array}{cccccccc}
1 & 1 & 1 & 1 & 1 & 1 & 1 & 1 \\
1 & -1 & 1 & -1 & 1 & -1 & 1 & -1 \\
1 & 1 & -1 & -1 & 1 & 1 & -1 & -1 \\
1 & -1 & -1 & 1 & 1 & -1 & -1 & 1 \\
1 & 1 & 1 & 1 & -1 & -1 & -1 & -1 \\
1 & -1 & 1 & -1 & -1 & 1 & -1 & 1 \\
1 & 1 & -1 & -1 & -1 & -1 & 1 & 1 \\
1 & -1 & -1 & 1 & -1 & 1 & 1 & -1 \\
\hline
8 & 0 & 0 & 0 & 0 & 0 & 0 & 0
\end{array}
$$

Figure 5.12 Multicode formed from a full set of length-8 Walsh Codes.

A simple proof for this is provided below:

Proof: Let $c_1, c_2, c_3, ..., c_N$ be the columns of a NxN matrix of either Walsh or Orthogonal Gold codes where each row is a code. Every row and column of this matrix is orthogonal to every other row and column [11]. The multicode is the superposition of all the codes of the matrix. So only the columns of the matrix are considered in this proof. Let C_{j_i} be the ith element of the jth column of the matrix. Since one column

of the matrix is composed of only 1s, without loss of generality, c_1 can be assumed to be the "all one" column. Then,

$c_1 = \{b_k\}$ where $b_k = 1$ for $k = 1$ to N. Then,

$$\sum_{i=1}^{N} c_{1_i} = N$$

Since every column is orthogonal to every other column including c_1,

$$\sum_{i=1}^{N} c_{1_i} . c_{2_i} = 0$$

$$\Rightarrow \sum_{i=1}^{N} c_{2_i} = 0 \qquad \because c_{1_i} = 1 \text{ for } i = 1 \text{ to } N$$

Similarly, it can proved that for any $j = 2$ to N,

$$\sum_{i=1}^{N} c_{j_i} = 0 \qquad \because \sum_{i=1}^{N} c_{1_i} . c_{j_i} = 0.$$

Hence the superposition of the entire set of a matrix of N orthogonal codes of length N where the $i = 1$ row consists of all 1s, results in a single code given by:

$a_i = N$ for $i = 1$ and

$= 0$ for $i = 2, 3, ..., N$.

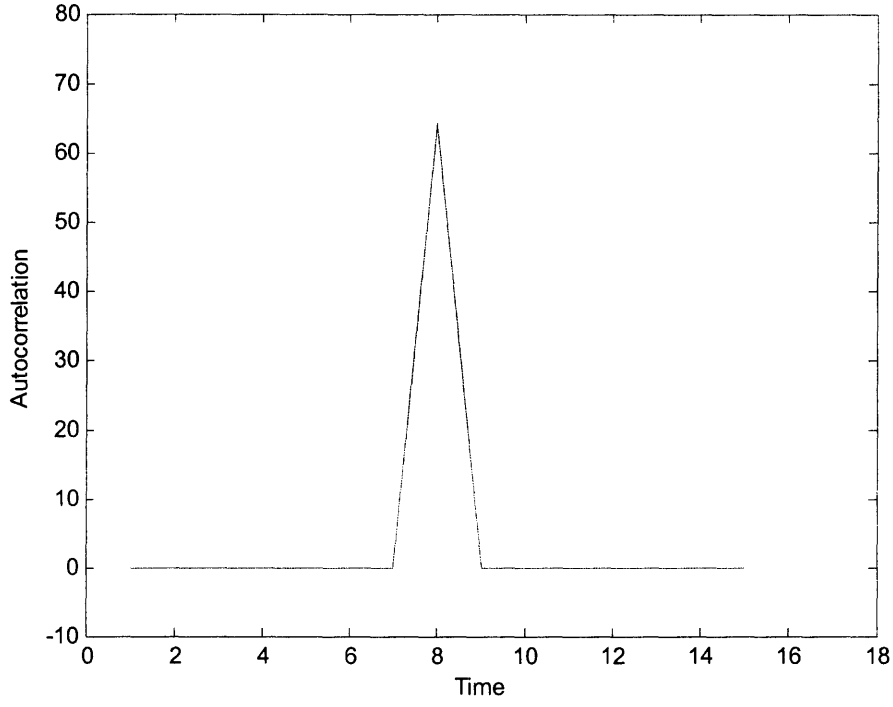

Figure. 5.13 Autocorrelation of a full-set length-8 Walsh multicode.

The autocorrelation of the multicode shown Figure 5.13 above will have a peak of $N^2 = 8^2 = 64$ at the main lobe and zero everywhere else.

The same is shown in Figure 5.14 for the full set of length 32 Walsh multicodes. In this case, the peak is $N^2 = 32^2 = 1024$. The width of the main lobe in each case is equal to the pulse width of the original code.

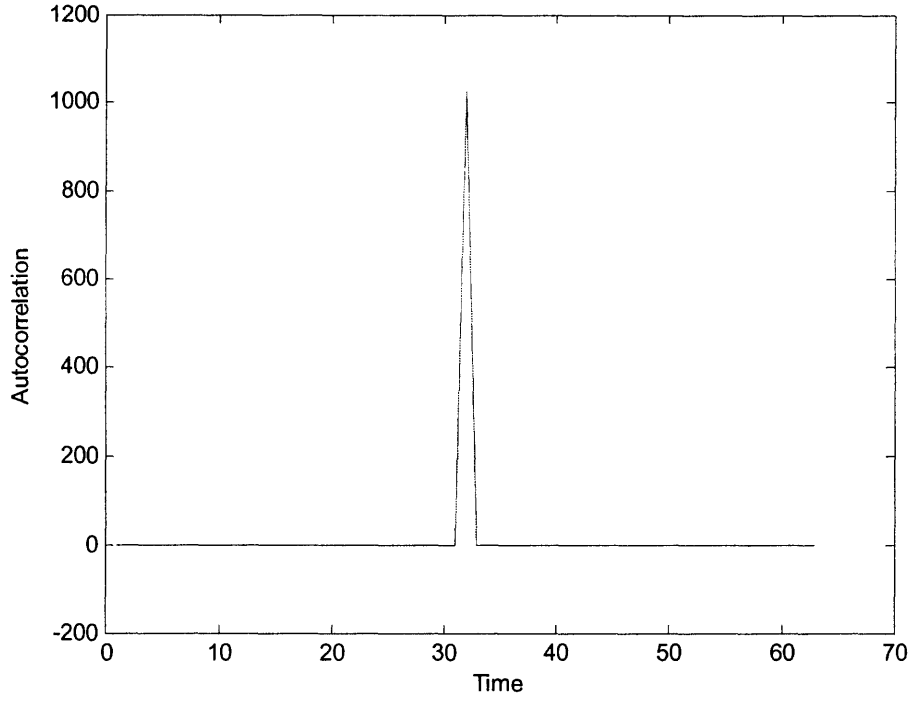

Figure. 5.14 Autocorrelation of a full-set length-32 Walsh multicode.

5.4 Trade-off in Multicode Radar Transmission

If the power limitation of the transmit amplifiers is taken into consideration, for the transmission of multicodes, the phased array should have the same number of transmit antennas as codes. This would prevent the peak power of the multicode from exceeding the power limitations of the amplifiers. Since the number of transmit antennas is limited by the complexity and manufacturing cost of the transmission system, there is a trade-off between the lowest PSLR that is required by the particular Radar application and the number of transmitters physically realizable and feasible in the Radar system.

As seen from the simulation results, the best 2-D ambiguity function is obtained when the entire set of orthogonal codes is used. Yet this also means that the number of

transmitting elements is the maximum for that particular code length. For small code lengths of 8 or 16, the number of antennas required may not be a problem and the best zero-Doppler ambiguity function can be obtained using multiple transmitters with no increase in PAPR.

CHAPTER 6

CONCLUSION AND FUTURE WORK

This thesis introduces the use of multicodes as Radar waveforms for improved range resolution through lower PSLR. It is shown that using multiple coded waveforms gives lower PSLR than existing Radar codes like Frank codes, when the number of codes used is large. In order to maintain the peak power of the multicodes within the limits of the amplifier specifications and avoid a high PAPR, each code should be transmitted from a separate antenna element in the phased array. This places a constraint on the amount of PSLR reduction that can be obtained because the number of transmit antennas will increase proportionally with the number of codes used. Yet, by using the entire set of orthogonal codes of small lengths like 8 or 16, it is possible to obtain a perfect zero-Doppler ambiguity function with no increase in PAPR (when compared to the single code case) if the number of antennas (8 or 16) is not a constraint in the radar system.

An extension of this work could be to consider certain combinations of Walsh codes of the same length which have very different bandwidths to enable multiple bandwidth codes within the same waveform. The potential use of this would be to realize multi-function Radar operations which require signals with different bandwidths to be transmitted simultaneously. Also, an analysis of the Doppler properties of these multicodes would be useful for further research on multicodes in Radar. Multicodes can also be used to obtain the angular resolution of targets that are spatially separated by implementing them in the Radar system described by Rabideau and Parker [13].

REFERENCES

[1] Skolnik, M.I. (1980). *Introduction To RADAR Systems* (2nd Ed). McGraw-Hill.

[2] Levanon, N. & Mozeson E (2004). *Radar Signals*. New Jersey: John Wiley and Sons.

[3] Levanon, N (1988). *RADAR Principles*. John Wiley and Sons.

[4] Rihaczek, A.W. (1969). *Principles of High Resolution RADAR*. McGraw Hill Inc.

[5] Woodward, P.M. (1980). *Probability and Information Theory with Applications to Radar*. Massachusetts: Artech House Inc.

[6] Nathanson, F.E. (1991) *RADAR Design Principles* (2nd Ed). McGraw Hill Inc.

[7] Sinsky, A.I. & Wang, C.P. (July 1974). Standardization of the Definition of the Radar Ambiguity Function. *IEEE Trans. on Aerospace and Elec. Sys.*

[8] Aghvami, A.H. (1994) Future CDMA Cellular Mobile Systems Supporting Multi-Service Operation. *PIMRC/WCN*

[9] Letaief, K.B., Chuang, J. C-I., & Murch, R.D. (13-17 Nov. 1995). Multicode High-Speed Transmission for Wireless Mobile Communications. *Global Telecommunications Conference GLOBECOM '95, IEEE, Vol. 3, 1835-1839.*

[10] Chih-Lin I & Gitlin, R.D. (1995). Multi-Code CDMA Wireless Personal Communications Networks. *IEEE International Conference on Communications ICC '95, Vol.2, 1060-1064.*

[11] Hanzo L., Munster, M., Choi B. J. & Keller T. (2003). *OFDM and MC-CDMA for Broadband Multi-User Communications, WLANs and Broadcasting*. John Wiley & Sons.

[12] Glisic, S. G. (2004). *Advanced Wireless Communications - 4G Technologies*. England: John Wiley & Sons Ltd.

[13] Rabideau, D.J., & Parker P. (Nov.2003) Ubiquitous MIMO Multifunction Digital Array Radar. *Thirty-Seventh Asilomar Conference on Signals, Systems and Computers, Vol. 1, 1057-1064.*

[14] Castoldi, P (2002). *Multiuser Detection in CDMA Mobile Terminals.* Massachusetts: Artech House Inc.

[15] Peterson, W.W and Weldon E. J., (1961). *Error Correcting Codes.* Cambridge MIT Press.

[16] Mahafza B. R. (1998). *Introduction To Radar Analysis.* CRC Press.

[17] Fishler E., Haimovich A., et al. (2004). Performance of MIMO Radar Systems: Advantages of Angular Diversity. *Thirty-eighth Asilomar Conference on Signals, Systems and Computers, Vol.1, 305-309.*

[18] Fishler E., Haimovich A., et al. (April 2004). MIMO Radar: An Idea Whose Time Has Come. *Proceedings of the IEEE Radar Conference, 71-78.*

[19] Cheng, R. G and Lin, P. (May 2000). OVSF Code Channel Assignment for IMT-2000. *Proceedings of the 51st IEEE Vehicular Technology Conference, Vol. 3, 2188-2192.*

[20] Tseng, Y. C. and Chao, C. M. (2002). Code Placement and Replacement Strategies for Wideband CDMA OVSF Code Tree Management. *IEEE Transactions on Mobile Computing, Vol. 1, No. 4, 293-302.*